Consensus-Based Odor Source Localization by Multiagent Systems Under Resource Constraints

Abhinav Sinha, *Member, IEEE*, Ritesh Kumar, Rishemjit Kaur, and Rajiv Kumar Mishra

***Abstract*—With advancements in mobile robot olfaction, networked multiagent systems (MASs) are used in odor source localization (OSL). These MASs are often equipped with small microprocessors that have limited computing capabilities, and they usually operate in a bandwidth and energy-constrained environment. The exigent need for a faster localizing algorithm under communication and computational resource constraints invites many design challenges. In this paper, we have designed a two-level hierarchical cooperative control strategy for heterogeneous nonlinear MASs for OSL. The agents are forced toward consensus expeditiously once the information on the whereabouts of the source is attained. The synthesis of the controller occurs in a hierarchical manner—obtaining a group decision, followed by resource-efficient robust control. Odor concentration and wind information have been used in a group decision-making layer to predict a probable location of the source as a tracking reference. This reference is then fed to the control layer that is synthesized using event-triggered sliding-mode control (SMC). The advantage of using event-triggered control scheduling in conjunction with the SMC is rooted in retaining the robustness of the SMC while lowering the resource utilization burden. Numerical simulations confirm the efficiency of the scheme put forth.**

***Index Terms*—Cooperative control, event-triggered sliding-mode control (SMC), heterogeneous nonlinear multiagent systems (MASs), inverse sine hyperbolic reaching law, odor source localization (OSL), robot olfaction.**

I. Introduction

ROBOT olfaction has gained prominence because this technique offers several advantages by deploying robotic agents. These agents are equipped to emulate sensing capabilities. From the forefront of engineering, several applications can be envisaged that demonstrate the significance of such robots [1]. First and foremost, these agents can be stationed where humans or animals, such as dogs, cannot be employed. Some common applications include locating oil spills and gas leaks, prevention of forest fires, identification of toxins [2]–[4], clearing unexploded remnants post war or after an armed conflict, etc. Due to the vast extent of application of this technique, a successful odor-localizing algorithm obligates synergistic integration of many disciplines of applied sciences. The multitude of simple and complex algorithms has been put forward for olfaction problems that mimic the practices of natural entities. However, studies have shown that probabilistic inference [5], [6]; robust control [7], [8]; swarm intelligence [9]–[11]; biased random walk [12]; and optimization-based and metaheuristic approaches are comparatively more successful in localization than bio-inspired techniques.

In the last couple of decades, odor localization has been targeted using chemical gradient-based approaches [13]–[16], a majority of which used a single robot system. Of all these techniques, the most widely used were chemotaxis [17]; anemotaxis [5], [18]; infotaxis [6]; and fluxotaxis [19]. These biomimetic approaches are computationally economical but have a low probability of success and are not time efficient. Multiagent systems (MASs), on the contrary, have become increasingly pervasive [20]–[22] due to obvious advantages of distributed sensing and actuation capabilities, increased feasibility and reliability, high efficacy and redundancy, increased probability of success, and higher robustness to local optima. In essence, odor localizing is a dynamical optimization task composed of the following subexercises—immediate plume sensing (plume identification), steering of the agents (plume traversal), and coordinated control of the agents [7].

Sandini *et al.* [23] proposed a robotic plume tracing strategy wherein agents computed temporally integrated differential gradients by using the instantaneous concentration measurements obtained from a pair of sensors, and used the information to move toward the region of higher concentration. Further, agents broadcasted their sensory data in a cooperative fashion such that the movement of each agent was affected by the indirect measure of concentration acquired from the neighbors, in addition to the self-measure of concentration. Hayes *et al.* [24] proposed a swarm intelligence-based distributed coordinated control technique and their experimental results established the fact that multiple agents perform more efficiently in localization than a single autonomous agent. In [25], cooperative mobile agents were designed using chemotaxis and a biased random walk. The agents exchanged information about their instantaneous positions and field strengths. This enabled the agents that have weak sensory data to adjust their heading according to the agents with a stronger

Manuscript received December 18, 2018; revised March 18, 2019 and May 27, 2019; accepted June 18, 2019. This work was supported in part by CSIR under Major Lab Project. This paper was recommended by Associate Editor G.-P. Liu. *(Corresponding author: Abhinav Sinha.)*

A. Sinha is with the Intelligent Systems and Control Laboratory, Department of Aerospace Engineering, Indian Institute of Technology Bombay, Mumbai 400076, India (e-mail: abhinavsinha@aero.iitb.ac.in).

R. Kumar and R. Kaur are with V1(b), Post-Harvest Technologies, CSIR-Central Scientific Instruments Organisation, Chandigarh 160030, India (e-mail: riteshkr@csio.res.in; rishemjit.kaur@csio.res.in).

R. K. Mishra is with the Department of Computer Science, School of Computing, Tokyo Institute of Technology, Tokyo 2268503, Japan (e-mail: mishra@sc.dis.titech.ac.jp).

Color versions of one or more of the figures in this paper are available online at http://ieeexplore.ieee.org.

Digital Object Identifier 10.1109/TCYB.2019.2924328

field and sensory data. In [26], agents used a bacterial-taxis strategy to localize the odor source. Fronczek and Prasad [27] proposed bio-inspired sensor swarms to detect leaks in pressurized systems. The sensory perception of the agents was based on the biological response of cockroaches and the communication architecture was modeled using the bee colony algorithm, while the self-repairing abilities were based on human decision making. Kennedy and Eberhart put forward particle swarm optimization (PSO) [28] in odor localization. Jatmiko *et al.* [29] utilized a modified PSO algorithm and electrical charge theory to locate the odor source by using neutral and charged robots. This prevented the robots from getting lured into false locations and local maximum concentrations. Simplified PSO was presented along with a distributed control by Lu *et al.* [30], which was essentially a type of *proportional-only* control scheme confining the operating region amidst the global and the local best. This technique often necessitates invoking intricate obstacle avoidance algorithms and subtle means to reduce high energy consumption.

Odor propagates in a nontrivial manner, causing fluctuations in measured concentrations. The downwind movement of odor molecules and the sense of wind direction dispense potent information about the relative location of the odor source. Hence, it is pragmatic to include wind information in the design of a controller. By using information on concentration and wind, Lu and Han [31] designed a particle filter-based coordinated control for the movement of a multirobot system toward an odor source. Lu *et al.* [30], [31] made a crude assumption of oversimplifying the dynamics of the agents to pure integrators while ignoring the adverse effect of external perturbations. Due to ubiquitous nonlinearity, such an assumption is not valid. Moreover, there are some classes of systems that cannot be stabilized via simple state feedback. Robust cooperative control protocols were designed in [7] and [32] for a homogeneous set of agents. In practice, it is strenuous to achieve a set of agents which are truly homogeneous. Even truly homogeneous agents show propensity toward heterogeneity over time and continued operation. A robust three-layered hierarchical approach in this area has been demonstrated in [33] for heterogeneous agents. Although the localization algorithm is fast, the authors assumed no limitations on the resources, such as computing power, bandwidth, etc.

Leveraging MASs increases the search performance of the task as agents rapidly exchange information among themselves. In a practical scenario, there is always some restriction on communication and computational capabilities. Nearly every scheme in odor localization has taken the available resources, such as computational and communication abilities, for granted. In [34], a probability PSO algorithm has been used in conjunction with an information-sharing matrix. The availability of faster algorithms for odor localization under practical constraints of actuation, energy, and bandwidth, still remains a challenge. This motivates a unified approach to communication, control, computing, and information technologies.

In this paper, we have attempted to synthesize a two-layered hierarchical cooperative control scheme. We call the first layer the *group decision making* layer, wherein the probable location of the source is determined by sensing the concentration of odor molecules and information of the wind. A measurement model [35] that describes the propagation of filaments can supply wind information, and agents provide concentration information by instantaneous plume sensing. In the MASs, one of the agents is deemed as the virtual leader and the others as followers. Depending on the data acquired, a suitable choice of the leader agent can be accomplished. The second layer is the robust cooperative control one, designed using an SMC implemented in an event-triggered fashion [36], [37]. In the second layer, the information attained in the first layer becomes the tracking reference for the controller. SMC [38], [39] provides robustness against uncertainties and finite-time convergence to the equilibrium point. Combining the advantages of SMC with event-triggered scheduling helps achieve robust finite-time control by exception; thereby, significantly reducing the burden on computation and communication. To the best of our knowledge, an event-triggered scheme has been applied to odor localization for the first time in the literature. The contributions of this paper can be summarized as follows.

Dynamic stabilization plays an important role in the synthesis of a controller. We have considered a set of heterogeneous agents with inherent nonlinearity which is more applicable in practice. Adjusting the functions in the system description, dynamics of a set of homogeneous agents, and that of pure integrators can be easily obtained. Utilizing a finite-time controller is not something out of the box, however, we have chosen a different perspective in the present discussions. The technique of SMC integrating a novel manifold and reaching law has been used in the localization of the odor source. Our prime motivation to use such a control lies in guaranteeing faster convergence, steady precision, and complete rejection of matched uncertainties. With an increase in the number of systems getting networked, the optimum utilization of communication bandwidth, computing resources, and energy expenses is paramount. The strategy we have adopted to address such issues is event-triggered control, wherein control authority is invoked only when the system demands it. This type of scheduling relaxes the controller at certain time instants. Consequently, robustness is guaranteed while lowering the computational and communication burden on the processor, and the processor can be used to execute various tasks in a time-sharing manner.

II. Mathematical Background

A. Spectral Graph Theory

We consider a directed graph topology $\mathcal{G} \coloneqq (\mathcal{V}, \mathcal{E}, \mathcal{A})$ represented by a node set $\mathcal{V} = \{1, 2, \ldots, N\}$, a directed edge set $\mathcal{E} = \{(i, j) \ \forall \ i, j \in \mathcal{V} \text{ and } i \neq j\}$, and an adjacency matrix $\mathcal{A} = a(i, j) \in \mathbb{R}^{N \times N}$. If the node $j \in \mathcal{E}$ supplies information to the node $i \in \mathcal{E}$, an edge $(i, j) \in \mathcal{E}$ is said to exist and nodes i and j are called neighbors. Physically, agents are modeled as nodes and their communication occurs over the edges in the digraph. Elements of the adjacency matrix $a(i, j)$ are non-negative. If $(i, j) \in \mathcal{E} \Rightarrow a(i, j) > 0$. If $(i, j) \notin \mathcal{E}$ or $i = j \Rightarrow a(i, j) = 0$. The degree matrix $\mathcal{D}$ is a diagonal matrix with entries $d_i \coloneqq \sum_{j=1}^{n} a(i, j)$. The Laplacian matrix

$\mathcal{L} \coloneqq \mathcal{D} - \mathcal{A}$ [40] is the key matrix in group consensus. When the leader node is connected to any other node via an edge, the corresponding entry of the incidence matrix $\mathcal{B}$ is 1; otherwise, it is 0. Note that the path between any two distinct nodes is not determined uniquely. A graph has a spanning tree if there exists at least one globally reachable node. Consequently, the matrix $\mathcal{H} = \mathcal{L} + \mathcal{B}$ has full rank [40].

B. Multiagent Dynamics and Problem Description

We consider heterogeneous leader-following the MASs of first order with inherent nonlinear dynamics connected in a directed topology. The information about the location of the odor source is not available globally, but via instantaneous plume sensing and local communication, the information is exchanged among the agents. The dynamics of the MASs comprised of N agents can be expressed mathematically as

$$\dot{x}_i(t) = f_i(x_i(t)) + u_{sm_i}(t) + \varsigma_i;\ i \in \{1, 2, \ldots, N\} \tag{1}$$

where $x_i(t)$ and $u_{sm_i}(t)$, respectively, represent the state and the control effort applied to agent i. $\varsigma_i(t)$ denotes the matched and bounded exogenous disturbances such that $\|\varsigma_i\| \leq \varsigma_{\max} < \infty$. The functions $f_i(\cdot)$ are assumed to satisfy Lipschitz continuity locally over a large compact domain with Lipschitz constant L_f. Further, we also assume that $f_i(\cdot)$ are input-to-state stable [41].

Remark 1: In (1), $f_i(\cdot) = f(\cdot) \Rightarrow$, the agents are homogeneous. For $f_i(\cdot) = 0$, dynamics of the MASs shapes into those of pure integrator systems.

If $x_s(t)$ denotes the probable location of the odor source and θ is a parameter that determines the accuracy with which the source declaration is made, then, we can describe our control objective in the following manner. The challenge of localizing an odor source using the MASs can be perceived as a cooperative control task warranting construction of control protocols $u_{sm_i}(t)$ such that the conditions $\lim_{t\to\infty} \|x_i - x_j\| = 0$ and $\lim_{t\to\infty} \|x_i - x_s\| \leq \theta$ are satisfied under minimum communication and computational resource utilization.

III. Synthesis of the Proposed Controller

We propose the following two-layered hierarchical cooperative control strategy to accomplish the odor-localizing task.

A. Group Decision Making

In order to make a prediction of the location of the odor source, concentration and wind information have been utilized. The probable source location (position) at any instant is then simply a weighted sum of this information

$$\phi(t) = \beta_1 p_i(t) + (1 - \beta_1) q_i(t). \tag{2}$$

A probable location of the odor source can be found by using concentration information alone [4], [42]. It is not so accurate since wind is decisive in shaping the odor plume [8], [33]. Intermittency and meandering of plume lead to irregular and chaotic flow. Low-resolution sensing data obtained from the measurement of odor concentration make it difficult to predict the probable location of the source. Wind provides effective information on the nature of plume and its propagation. The sparse and stochastic nature of plume also complicates the plume traversal since a simple sequential search cannot be applied. Plume traversal also requires specialized trajectory behavior—to progress toward the global maxima, to maintain contact with the plume, and to reorient the heading toward plume (leading to the global maxima) when the contact is lost. The mean concentration information decreases with an increase in distance from the source. As agents progress upstream toward the source, plumes become more sparse due to intermittency in odor packets and sensory information becomes very less in resolution. Under such a scenario, maintaining contact with the plume and an exchange of local information becomes difficult. Disregarding wind information leads to lower success rates and larger localization time. Hence, we have included the effects of wind, along with the concentration information to enhance the localization performance.

In the context of PSO, $p_i(t)$ in (2) is called the oscillation center. $q_i(t)$ captures information of the wind. $\beta_1 \in (0, 1)$ denotes the coefficient weight, and ϕ becomes the reference sent to the controller for accurate tracking. We now discuss insights on obtaining $p_i(t)$ and $q_i(t)$.

For initialization, we shall make use of continuous-time PSO. Although PSO is widely encountered in discrete time, the trajectory of the particles (or agents) is smooth and continuous in nature. The trajectory does not exhibit discrete jumps from one position to another. Hence, PSO performance may be boosted using a continuous-time equivalent. Thus, continuous-time PSO [43] can be described by the following differential equation:

$$\ddot{x}_i(t) + (1 - \omega)\dot{x}_i(t) + \alpha x_i(t) = \alpha_1 x_l(t) + \alpha_2 x_g(t). \tag{3}$$

In (3), $\alpha = \alpha_1 + \alpha_2$, and initial conditions $x_i(0) = x_0$ and $\dot{x}_i(0) = v_0$. With ω as the inertia factor, and $v_i(t)$ and $x_i(t)$ representing the respective velocity and position of the ith agent, the algorithm can be used as a *proportional-only* control law in itself, and can be expressed as

$$u_{\mathrm{PSO}}(t) = \alpha_1(x_l(t) - x_i(t)) + \alpha_2\big(x_g(t) - x_i(t)\big). \tag{4}$$

In (4), $x_l(t)$ is the previous best position and $x_g(t)$ is the global best position of the neighbors of the ith agent at any given time t. The acceleration coefficients are represented by α_1 and α_2. Via local communication, every member of the swarm can acquire some information about the magnitude of odor concentration. From this, it is easy to compute the position of the agent with the global best. The oscillation center $p_i(t)$ can be further computed as

$$p_i(t) = \frac{\alpha_1 x_l(t) + \alpha_2 x_g(t)}{\alpha_1 + \alpha_2}. \tag{5}$$

Thus, from (4) and (5)

$$u_{\mathrm{PSO}}(t) = (\alpha_1 + \alpha_2)\{p_i(t) - x_i(t)\} = \alpha\{p_i(t) - x_i(t)\} \tag{6}$$

which, in essence, is a *proportional-only* controller with proportional gain α. However, due to limitations, such as premature convergence, swarm disordering, etc., (4) is not used as the main control law.

Now, computing $q_i(t)$ remains to obtain the probable location of the source. A single filament is composed of several

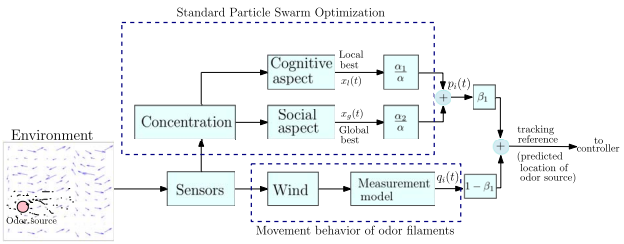

Fig. 1. Group decision making when determining odor source location.

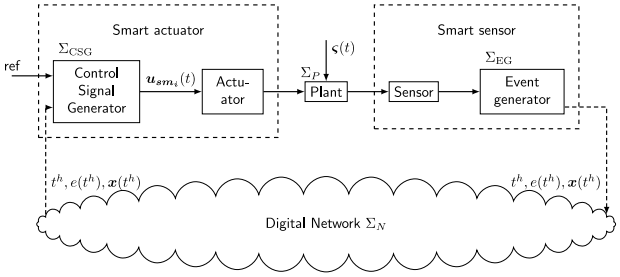

Fig. 2. Illustration of event-triggered control.

odor molecules. Let $x_f(t)$ denote the filament's position at time t and the mean airflow velocity be denoted as $\bar{v}_a(t)$. Due to many environmental factors, the information is usually corrupted with some noise. Let $n(t)$ denote the random process in the model. We now model the movement behavior of a single filament [35] as follows:

$$\dot{x}_f(t) = \bar{v}_a(t) + n(t). \tag{7}$$

Without compromising generality, we denote $t = 0$ as the time when the experiment starts. From (7), we have

$$x_f(t) = \int_0^t \bar{v}_a(\tau)d\tau + \int_0^t n(\tau)d\tau + x_f(0) \tag{8}$$

where $x_f(0)$ represents the initial position of odor filaments. The odor molecules, or filaments, are released from the odor source, so the position of filaments at $t = 0$ is the same as the initial source location $x_s(0)$, that is

$$x_f(t) = \int_0^t \bar{v}_a(\tau)d\tau + \int_0^t n(\tau)d\tau + x_s(0). \tag{9}$$

Note that $x_s(0)$ signifies the actual source position at $t = 0$. To simplify the problem a little bit, we can safely assume that there is only one stationary source. Thus, $x_s(t) = x_s(0)$. Hence

$$x_f(t) = x_s(t) + \bar{v}_a^\star(t) + w^\star(t). \tag{10}$$

In (10), $\int_0^t \bar{v}_a(\tau)d\tau = \bar{v}_a^\star(t)$ and $\int_0^t n(\tau)d\tau = w^\star(t)$. From (10)

$$x_f(t) - \bar{v}_a^\star(t) = x_s(t) + w^\star(t). \tag{11}$$

Relationship (11) is nothing but the position information of the source $x_s(t)$ corrupted by some noisy parameter $w^\star(t)$. Hence

$$q_i(t) = x_s(t) + w^\star(t). \tag{12}$$

Therefore, the tracking reference ϕ in (2) can now be constructed from (5) and (12). A simple block schematic has been presented in Fig. 1 to illustrate the prediction of source location.

Agents instantaneously sense the plume and the environment for clues on the odor source. Note that the MASs under consideration are a leader-following type. Since every agent detects some information at some time, the agent with maximum information is chosen as the leader.

B. Resource-Efficient Cooperative Control

In this part, we discuss the synthesis of a robust controller that attempts to track the reference (2) in order to localize the source. Leveraging MASs increases the probability of success, but adds to the overall economy. Agents exchange their information via local sensing and communication, and there is a cost to maintain these links. In practice, agents are often equipped with small computing devices and have to operate under constraints, such as limited bandwidth, on-board processing power, etc. Event-triggered scheduling of control has gained prominence in such settings [44], [45]. Conventional sampled-data scheduling considers updating the controller in a periodic fashion even after the control objective has been achieved. Continuous transmission, sampling, and CPU occupancy to carry on computations even when the signal shows less variations overtax the resources. An efficient way is to sample only when the local measurement error exceeds some threshold (the range in which the system may tolerate fluctuations). Event-triggered control can be used to abandon periodic sampling and the control update in exchange for a deliberate one to improve resource efficiency. The prime motivation to use the proposed event-driven technique stems from the objective to adapt the utilization of elements in a control loop to the current needs. A diagram illustrating event-based control is shown in Fig. 2.

Further, event-triggered sampling has to be combined with a robust control technique so that finite-time localization is achieved under resource constraints. SMC is one such scheme avowed for its inherent robustness, dynamic stabilization of uncertain systems, and ability to reject a particular class of uncertainty. A consequence of combining SMC with an event-triggered strategy is to retain the measure of robustness in the system and, at the same time, achieve reduction in computational expense [46], [47].

Denote the tracking error vector as

$$e_i(t) = x_i(t) - \phi(t);\ t \in \left[t^h, t^{h+1}\right). \tag{13}$$

The topological error vector can be defined as

$$\epsilon_i(t) = \mathcal{H}e_i(t) = \mathcal{H}(x_i(t) - \phi(t)). \tag{14}$$

In SMC, design of the sliding manifold is directly linked to system performance. In linear manifolds, the control authority required to achieve sliding motion is directly proportional to the magnitude of error. If actuator constraints are to be respected, control is usually hard upper and lower bounded.

This renders the manifold attractive only in part, which is known as the sliding regime. Stability as well as desired performance outside this portion are not guaranteed. Further, the controller is susceptible to saturation if the tracked variable is not closer to the present value of the state. In such cases, the controller fails to cope up and the system may tend toward instability. It is thus advantageous to utilize nonlinear manifolds with the ability to hold the states of the system despite where they are in the state space. We propose a nonlinear manifold

$$s_i(t) = \lambda_1 \tanh(\lambda_2 \epsilon_i(t)) \tag{15}$$

offering faster reachability of state trajectories to the manifold. $\lambda_1 \in \mathbb{R}^+$ represents the convergence speed toward the proposed sliding manifold, and $\lambda_2 \in \mathbb{R}^+$ denotes the slope of the manifold. The dynamics of the manifold for such consideration is chosen as

$$\dot{s}_i(t) = -\mu \sinh^{-1}(m + w|s_i(t)|)\text{sign}(s_i(t)). \tag{16}$$

In (16), w denotes the gain of the controller. To ensure that the argument of $\sinh^{-1}(\cdot)$ is a finite positive quantity, m is used as a small offset. In general, $0 < m << w$, and μ is a parameter that aids in additional tuning of the gain.

Thus, the overall gain factor of the novel reaching law (16) becomes $\mu \sinh^{-1}(m + w|s_i(t)|)$, which is nonlinear. This aids in rapid convergence toward the sliding manifold. This reaching law is smooth and does not oscillate at very high frequencies; hence, it can be used to safely operate mechatronic systems.

Theorem 1: Consider the MASs dynamics (1) under a directed topological interaction, tracking errors (13), (14), and the sliding manifold (15). The stabilizing event-triggered SMC protocols that ensure accurate reference tracking in a resource-efficient manner and drive the agents toward agreement can be expressed as

$$u_{sm_i}(t) = -\Big\{(\Lambda\mathcal{H})^{-1}\mu \sinh^{-1}\Big(m + w\Big|s_i\Big(t^h\Big)\Big|\Big)\text{sign}\Big(s_i\Big(t^h\Big)\Big)\Gamma^{-1} + \Big(f\Big(x_i\Big(t^h\Big)\Big) - \dot{\phi}\Big(t^h\Big)\Big)\Big\} \tag{17}$$

where $\Lambda = \lambda_1\lambda_2$, $\Gamma = 1 - \tanh^2(\lambda_2\epsilon_i(t))$, $w > \sup_{t\geq 0}\{\|\varsigma_i\|\}$, and $\mu > \sup\{\|\Lambda\mathcal{H}\varsigma_i\Gamma\|\}$. $t = t^h$ denotes the instants when control is executed.

Remark 2: As mentioned earlier, $\lambda_1, \lambda_2 \in \mathbb{R}^+$, which implies $\Lambda \neq 0$. The argument of $\tanh(\cdot)$ satisfies $\lambda_2\epsilon_i(t) \neq \pi\iota(\kappa + 1/2)$ for $\kappa \in \mathbb{Z}$ since it is always finite. Thus, Γ is also invertible. Moreover, the presence of at least one globally reachable node implies that $\mathcal{H}^{-1}$ exists.

Proof: From (14) and (15), we can proceed as follows:

$$\dot{s}_i(t) = \lambda_1\Big\{\lambda_2\dot{\epsilon}_i(t)\Big(1 - \tanh^2(\lambda_2\epsilon_i(t))\Big)\Big\} \tag{18}$$

$$= \lambda_1\lambda_2\dot{\epsilon}_i(t) - \lambda_1\lambda_2\dot{\epsilon}_i(t)\tanh^2(\lambda_2\epsilon_i(t)) \tag{19}$$

$$= \lambda_1\lambda_2\dot{\epsilon}_i(t)\Big\{1 - \tanh^2(\lambda_2\epsilon_i(t))\Big\} \tag{20}$$

$$= \Lambda\mathcal{H}\big(\dot{x}_i(t) - \dot{\phi}(t)\big)\Gamma \tag{21}$$

where Λ and Γ have been defined in Theorem 1. From (1), we can further simplify (21) as

$$\dot{s}_i(t) = \Lambda\mathcal{H}\big(f(x_i(t)) + u_{sm_i}(t) + \varsigma_i - \dot{\phi}(t)\big)\Gamma. \tag{22}$$

By virtue of (16), the control authority that forces the state trajectories toward the switching hyperplane is

$$u_{sm_i}(t) = -\Big\{(\Lambda\mathcal{H})^{-1}\mu \sinh^{-1}(m + w|s_i(t)|)\text{sign}(s_i(t))\Gamma^{-1} + \big(f(x_i(t)) - \dot{\phi}(t)\big)\Big\} \tag{23}$$

which is the SMC protocol without an event-triggered strategy. Discretization of the law (23) results in (17), thereby completing the proof. ■

Remark 3: Control protocol (17) does not contain the uncertainty term. Hence, it can be practically implemented.

It is very momentous to investigate the necessary and sufficient conditions for the existence of sliding motion when the protocol (17) is invoked. Note that we consider the system to be executing sliding motion if for any time $t_1 \in [0, \infty)$, state trajectories are ushered toward the manifold $s_i(t) = 0$ and are maintained thereafter.

Theorem 2: Consider the system described by (1), tracking errors (13), (14), sliding manifold (15), and the control protocol (17). Sliding mode will exist in close proximity of (15) if state trajectories originating outside (15) are continuously driven by the protocol (17) toward (15) and are maintained thereafter. This is so called the reachability condition, which is warranted for some reachability constant $\eta > 0$. Further, stability can also be ascertained in the sense of Lyapunov if gain μ is selected as $\mu > \sup\{\|\Lambda\mathcal{H}\varsigma_i\Gamma\| + \|\Lambda\mathcal{H}\|L_f\|\Xi(t)\|\|\Gamma\|\}$, where

$$\Xi_i = x_i\Big(t^h\Big) - x_i(t) \tag{24}$$

is the error introduced due to discretization of the protocol (17).

Proof: Let us choose a Lyapunov function candidate

$$V_i = 0.5s_i^2. \tag{25}$$

Computing the derivative of (25) along system trajectories yields

$$\dot{V}_i = s_i\dot{s}_i \tag{26}$$

$$= s_i\big\{\Lambda\mathcal{H}\big(f(x_i(t)) + u_{sm_i}(t) + \varsigma_i - \dot{\phi}(t)\big)\Gamma\big\}. \tag{27}$$

Substituting (17) into (27) gives

$$\begin{aligned}\dot{V}_i &= s_i(t)\Big(-\mu \sinh^{-1}\Big(m + w\Big|s_i\Big(t^h\Big)\Big|\Big)\text{sign}\Big(s_i\Big(t^h\Big)\Big) + \Lambda\mathcal{H}\varsigma_i\Gamma + \Lambda\mathcal{H}\Big\{f_i(x_i(t)) - f_i\Big(x_i\Big(t^h\Big)\Big)\Big\}\Big)\\ &\leq \|s_i(t)\|\Big\{\|\Lambda\mathcal{H}\|L_f\Big\|x_i(t) - x_i\Big(t^h\Big)\Big\|\|\Gamma\| + \|\Lambda\mathcal{H}\varsigma_i\Gamma\| - \mu \sinh^{-1}\Big(m + w\Big|s_i\Big(t^h\Big)\Big|\Big)\text{sign}\Big(s_i\Big(t^h\Big)\Big)\Big\}\\ &\leq \|s_i(t)\|\Big\{\|\Lambda\mathcal{H}\|L_f\|\Xi(t)\|\|\Gamma\| + \|\Lambda\mathcal{H}\varsigma_i\Gamma\| - \mu \sinh^{-1}\Big(m + w\Big|s_i\Big(t^h\Big)\Big|\Big)\text{sign}\Big(s_i\Big(t^h\Big)\Big)\Big\}.\end{aligned} \tag{28}$$

Remark 4: $\forall t \in [t^h, t^{h+1})$, $\text{sign}(s_i(t)) = \text{sign}(s_i(t^h))$ holds whenever $s_i(t) > 0$ or $s_i(t) < 0$.

Thus, in the immediate outside vicinity of the manifold

$$\begin{aligned}\dot{V}_i &\leq \Big\{\|s_i(t)\|\|\Lambda\mathcal{H}\|L_f\|\Xi(t)\|\|\Gamma\| + \|s_i(t)\|\|\Lambda\mathcal{H}\varsigma_i\Gamma\| \\ &\qquad - \mu\sinh^{-1}\Big(m + w\Big|s_i\Big(t^h\Big)\Big|\Big)\|s_i(t)\|\Big\} \\ &\leq -\eta\|s_i(t)\| \end{aligned} \tag{29}$$

where $\eta = \mu\sinh^{-1}(m + w|s_i(t^h)|) - \|\Lambda\mathcal{H}\varsigma_i\Gamma\| - \|\Lambda\mathcal{H}\|L_f\|\Xi(t)\|\|\Gamma\| > 0$ is called the reachability constant, and $\mu > \sup\{\|\Lambda\mathcal{H}\varsigma_i\Gamma\| + \|\Lambda\mathcal{H}\|L_f\|\Xi(t)\|\|\Gamma\|\}$. This is evidence that the switching surface is an attractor, and state trajectories have a tendency to decrease toward it $\forall t \in [t^h, t^{h+1})$. The discretization error (24) vanishes at instants $t = t^h$. Therefore, $s_i(t) = 0$ and $t = t^h$ imply

$$\dot{V}_i < 0 \tag{30}$$

which proves the stability in the sense of Lyapunov.

Remark 5: The switching manifold is a global attractor, as seen from the implications in (16) and (29), and the conditions $\mu > 0$, $\|s_i\| > 0$, and $\sinh^{-1}(\cdot) > 0$.
Thus, from the preceding discussions, closed-loop stability follows, and the proof is complete. ■

Remark 6: The triggering rule characterizes the event-firing instants t^h. Until the arrival of the next sample, the control authority is maintained at its previous value.

Proposition 1: We propose a novel dynamic event triggering rule in (31) that depends not only on local measurement error but also on its derivative

$$\rho = \varrho_1\epsilon_i(t) + \varrho_2\dot{\epsilon}_i(t)^2 - \big(\zeta_0 + \zeta_1 e^{-\xi t}\big). \tag{31}$$

In (31), $\varrho_1 > 0$, $\varrho_2 > 0$, $\zeta_0 \geq 0$, $\zeta_1 \geq 0$, $\zeta_0 + \zeta_1 > 0$, and $\xi \in (0, 1)$. Whenever $\rho > 0$, that is, $\varrho_1\epsilon_i(t) + \varrho_2\dot{\epsilon}_i(t)^2 > (\zeta_0+\zeta_1 e^{-\xi t})$, the sample is taken and the controller is updated. The triggering rule (31) can be written iteratively as

$$t_i^{h+1} = \inf\Big\{t_i^h \in \Big[t_i^h, \infty\Big) : \rho > 0\Big\}. \tag{32}$$

Remark 7: The term $(\zeta_0 + \zeta_1 e^{-\xi t})$ varies with time in an exponential manner, but is independent of the states. This prevents the accumulation of samples at the same time. In other words, unchecked discrete transitions within a time segment that is finite and bounded (also known as *Zeno* behavior) [48], [49] are excluded.

Using such a threshold is advantageous as communication with the neighbors can be abstained. The decision to invoke communication from the sensor to actuator can be attributed to this threshold in the rule (32).

Remark 8: Most practical scenarios necessitate that the threshold should not be fixed permanently. Consider a group of agents in certain geometrical formation, wherein an interagent information exchange must be maintained even after they have attained the formation. If the threshold remains fixed, some data packets on the prescribed geometry might not trigger.

Zeno phenomenon defeats the very reason to reduce the burden on computational and communication resources in a hybrid system. An adverse consequence of this phenomenon is that the global solutions cease to exist for all time. The separation of adjacent samples in time by a finite positive quantity in all possible scenarios, including unknown disturbances, modeling uncertainties, parameter inaccuracies, etc., ensures that the aforementioned adverse situation never arises.

Theorem 3: Consider the system described by (1), the proposed control authority (17), and the discretization error (24). The sequence of triggering instants $\{t_i^h\}_{h=0}^{\infty}$ respects the triggering rule (31) and guarantees that the interevent execution time T_i^h is bounded below by a finite positive quantity ϖ, where

$$\varpi = \frac{1}{L_f}\ln\left(1 + \frac{\|\Xi_i(t)\|_\infty}{\Omega\big(\big\|x_i\big(t^h\big)\big\|\big) + \big\|\dot{\phi}\big(t^h\big)\big\| + \varkappa}\right). \tag{33}$$

Consequently, *Zeno* phenomenon is excluded, that is, samples do not accumulate at the same instant.

Proof: The discretization error is nonzero between successive sampling moments. $T_i^h = t_i^{h+1} - t_i^h$ is the time it takes the discretization error to rise from 0 to $\|\Xi_i\|_\infty$. Thus

$$\begin{aligned}\frac{d}{dt}\|\Xi_i(t)\| \;&\leq\; \left\|\frac{d}{dt}\Xi_i(t)\right\| \leq \left\|\frac{d}{dt}x_i(t)\right\| \\ &\Rightarrow \left\|\frac{d}{dt}\Xi_i(t)\right\| \leq \big\|f(x_i(t)) + u_{sm_i} + \varsigma_i\big\|. \end{aligned} \tag{34}$$

From (17), we can further simplify (34) as

$$\begin{aligned}\left\|\frac{d}{dt}\Xi_i(t)\right\| &\leq \Big\|-(\Lambda\mathcal{H})^{-1}\mu\sinh^{-1}\Big(m + w\Big|s_i\Big(t^h\Big)\Big|\Big) \\ &\qquad \times \operatorname{sign}\Big(s_i\Big(t^h\Big)\Big)\Gamma^{-1} + f(x_i(t)) - f\Big(x_i\Big(t^h\Big)\Big) \\ &\qquad + \varsigma_i\dot{\phi}\Big(t^h\Big)\Big\| \\ &\leq L_f\|x_i(t)\| + L_f\Big\|x_i\Big(t^h\Big)\Big\| + \|\varsigma_i\| + \Big\|\dot{\phi}\Big(t^h\Big)\Big\| \\ &\quad + \Big\|(\Lambda\mathcal{H})^{-1}\Big\|\mu\Big\|\sinh^{-1}\Big(m + w\Big|s_i\Big(t^h\Big)\Big|\Big)\Big\|\Big\|\Gamma^{-1}\Big\| \\ &\leq L_f\Big\|x_i\Big(t^h\Big) + \Xi_i(t)\Big\| + L_f\Big\|x_i\Big(t^h\Big)\Big\| + \|\varsigma_i\| \\ &\quad + \Big\|\dot{\phi}\Big(t^h\Big)\Big\| \\ &\quad + \Big\|(\Lambda\mathcal{H})^{-1}\Big\|\mu\Big\|\sinh^{-1}\Big(m + w\Big|s_i\Big(t^h\Big)\Big|\Big)\Big\|\Big\|\Gamma^{-1}\Big\| \\ &\leq L_f\|\Xi_i(t)\| + 2L_f\Big\|x_i\Big(t^h\Big)\Big\| + \|\varsigma_i\| + \Big\|\dot{\phi}\Big(t^h\Big)\Big\| \\ &\quad + \Big\|(\Lambda\mathcal{H})^{-1}\Big\|\mu\Big\|\sinh^{-1}\Big(m + w\Big|s_i\Big(t^h\Big)\Big|\Big)\Big\|\Big\|\Gamma^{-1}\Big\| \\ &\leq L_f\|\Xi_i(t)\| + \Omega\Big(\Big\|x_i\Big(t^h\Big)\Big\|\Big) + \varkappa + \Big\|\dot{\phi}\Big(t^h\Big)\Big\|. \end{aligned} \tag{35}$$

In (35), $\|\dot{\phi}(t^h)\|$, $\Omega(\|x_i(t^h)\|) = 2L_f\|x_i(t^h)\|$, and $\varkappa = \|(\Lambda\mathcal{H})^{-1}\|\mu\|\sinh^{-1}(m+w|s_i(t^h)|)\|\|\Gamma^{-1}\| + \|\varsigma_i\|$ are all positive quantities. The solution to (35) $\forall t \in [t^h, t^{h+1})$ with initial condition $\|\Xi_i(t^h)\| = 0$ can be given as

$$\|\Xi_i(t)\| \leq \frac{\Omega\big(\big\|x_i\big(t^h\big)\big\|\big) + \big\|\dot{\phi}\big(t^h\big)\big\| + \varkappa}{L_f}\Big(e^{L_f(t_i - t_i^h)} - 1\Big). \tag{36}$$

At $t = t^{h+1}$

$$\begin{aligned}\|\Xi_i(t)\|_\infty &= \Big\|\Xi_i\Big(t^{h+1}\Big)\Big\| \\ &\leq \frac{\Omega\big(\big\|x_i\big(t^h\big)\big\|\big) + \big\|\dot{\phi}\big(t^h\big)\big\| + \varkappa}{L_f}\Big(e^{L_f T_i^h} - 1\Big). \end{aligned} \tag{37}$$

Computing T_i^h from (37), gives

$$T_i^h \geq \frac{1}{L_f}\ln\left(1+\frac{\|\Xi_i(t)\|_\infty}{\Omega\left(\left\|x_i\left(t^h\right)\right\|\right)+\left\|\dot{\phi}\left(t^h\right)\right\|+\varkappa}\right) \tag{38}$$

which is the same as ϖ given in (33). From (37), it is easy to verify that the interevent execution time is bounded below by a finite positive quantity, making the triggers admissible. The proof is completed. ■

IV. Results of Numerical Simulation

Odor molecules have a tendency to heavily disperse in a diffusion-characterized environment. However, the assumption that an environment is dominated by diffusion is a very strong one and ignores several factors. A situation that is relatively closer to reality must accommodate thermal effects, effects of wind, and turbulence diffusion. Unfortunately, the effects of turbulence are onerous to model. In addition, environmental characteristics can also be illustrated by advection phenomenon. In this paper, we have regarded a diffusion–advection plume model. Further, it has also been assumed that the airflow is uniform in the domain of localization for all time. It is worth noting that the coefficient of turbulence diffusion (K) should be known in advance by virtue of some suitable measurements. If this is not the case, then this coefficient must be estimated or correlated as a function of wind velocity, that is, $K = f(v_a)$. This correlation can be carried out online with the obtained measurements (e.g., output from anemometers and gas sensors, etc.). We recall the diffusion–advection model presented in [22] and [50] to simulate the dynamic odor plume under disturbances that are time varying but bounded. A steady concentration profile for a very large span of time ($t \to \infty$) is given by

$$C(\vec{\boldsymbol{r}},\infty) = \frac{q_0}{2\pi K d_i}\exp\left\{-\frac{v_a}{2K}(d_i - \vec{\boldsymbol{r}} + \vec{\boldsymbol{r}}_0)\right\}. \tag{39}$$

In (39), $\vec{\boldsymbol{r}}_0 = x_s(t)$ denotes the odor source coordinates, $d_i = \|x_i - x_s\|$, q_0 is the rate of filament release, and K is the coefficient of turbulent diffusion that does not depend on the diffusing material.

We shall test the proposed algorithm on a set of heterogeneous agents operating under communication constraints. For brevity, we shall consider that the MASs consist of five agents in a directed topology as shown in Fig. 3. Dynamics of the MASs have been taken as

$$\dot{x}_1 = 0.1\sqrt[3]{\sin(x_1)} + \cos(2\pi t) + u_{sm_1}(t) + \varsigma_1(t) \tag{40}$$
$$\dot{x}_2 = 0.1\sin(x_2) - \cos\left(e^{-x_2 t}\right) + u_{sm_2}(t) + \varsigma_2(t) \tag{41}$$
$$\dot{x}_3 = 0.1\sqrt[3]{\sin(x_3)} + \cos^2(2\pi t) + u_{sm_3}(t) + \varsigma_3(t) \tag{42}$$
$$\dot{x}_4 = 0.1\sin(x_4) + \cos(x_4) + u_{sm_4}(t) + \varsigma_4(t) \tag{43}$$
$$\dot{x}_5 = 0.1\cos(x_5) - \cos(2\pi t) - e^{-t} + u_{sm_5}(t) + \varsigma_5(t). \tag{44}$$

In this topology, agent 1 acts as a virtual leader, and the arrows denote the direction of information flow. By local interaction, a consensus is established in finite time. The localization grid is taken to be 100 × 100 m^2. The localization accuracy parameter (θ) represents the distance from the true odor source within which the MASs should be for the source to be declared as found. For simulation, we shall take $\theta = 0.001$, and the maximum mean airflow velocity ($\bar{v}_{a_{\max}}$) in the grid of localization has been chosen to be 1 m/s. The acceleration coefficients α_1 and α_2 have been chosen to be equal to maintain a balance between the grouping ability and

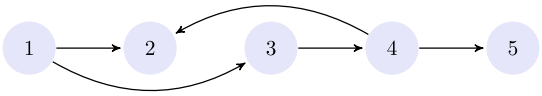

Fig. 3. Interaction topology of agents.

TABLE I
Localization Scenarios

Scenario	Group Consensus	Parallel Formation	No perturbation	Matched perturbations
Scenario 1	✓	×	✓	×
Scenario 2	×	✓	✓	×
Scenario 3	✓	×	×	✓
Scenario 4	×	✓	×	✓

TABLE II
Localization Performance Metrics

Technique	Average Success rate	Median localization Time	Control Implementation
Scenario 1 (present work)	100%	19.00 sec	Time-triggered
Scenario 2 (present work)	100%	22.70 sec	Time-triggered
Scenario 3 (present work)	100%	21.50 sec	Time-triggered
Scenario 4 (present work)	100%	28.00 sec	Time-triggered
Scenario 1 (present work)	100%	21.50 sec	Event-triggered
Scenario 2 (present work)	100%	24.10 sec	Event-triggered
Scenario 3 (present work)	100%	22.00 sec	Event-triggered
Scenario 4 (present work)	100%	26.00 sec	Event-triggered
APF-PSO [10]	93%	89.74 sec	Time-triggered
PSO [51]	21.5%	986.25 sec	Time-triggered
CPSO [29]	20.4%	926.00 sec	Time-triggered
BBPSO [11]	83.2%	700.00 sec	Time-triggered
P-PSO [34]	94.8%	544.00 sec	Time-triggered
FTMCS [8]	100%	137.50 sec	Time-triggered

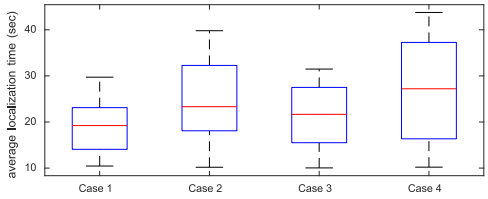

Fig. 4. Average localization time for the four scenarios under time-triggered control.

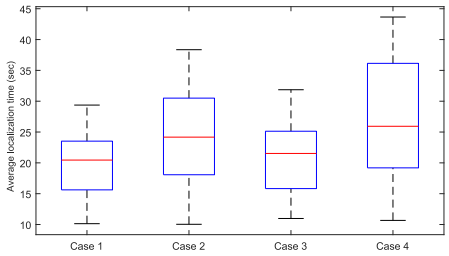

Fig. 5. Average localization time for the four scenarios under event-triggered control.

TABLE III
Number of Controller Updates for the Proposed Control Scheme

Agent	Agent 1	Agent 2	Agent 3	Agent 4	Agent 5	
No. of event-triggered control updates	326	272	488	247	171	
No. of time-triggered control updates	1000	1000	1000	1000	1000	
Percentage of reduction in control updates	67.4	72.8	51.2	75.3	82.9	
Total number of effective control updates						1504
Effective percentage of reduction in control updates						69.92

TABLE IV
SIMULATION PARAMETERS

β_1	ω_{max}	α_1	α_2	λ_1	λ_2	μ	m	w	ϱ_1	ϱ_2	ζ_0	ζ_1	ξ	K	q_0	ς_{max}
0.5	2 rad/s	0.25	0.25	1.572	3.61	9.65	10^{-3}	2	0.8	0.6	10^{-4}	0.2278	0.57	0.02 m^2/sec	2 mg/sec	2.47

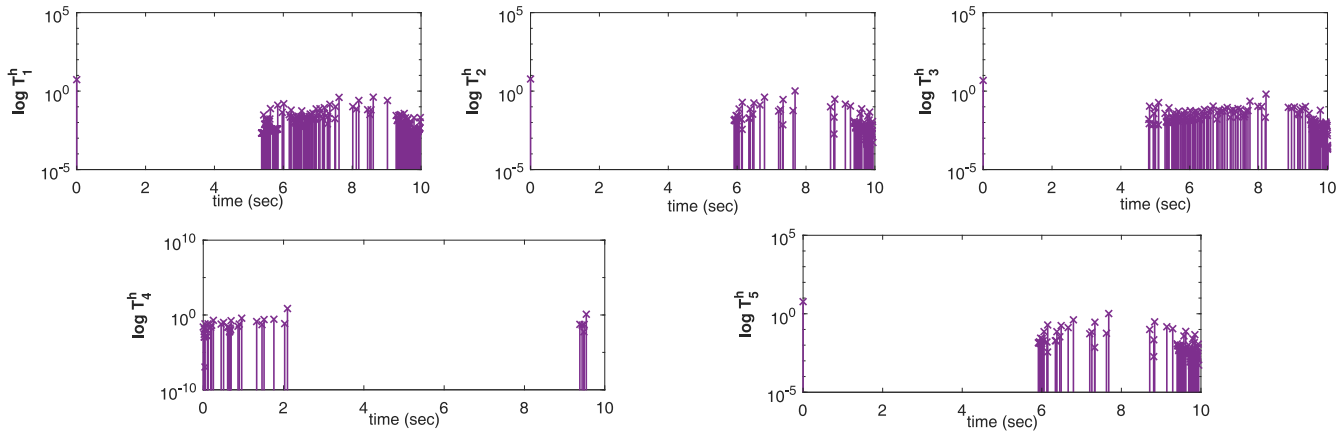

Fig. 6. Sampling intervals of agents.

group convergence. Similarly, equal weights have been chosen to construct the tracking reference from the information from wind and concentration. A suitable choice of inertia weight is required in PSO to maintain a tradeoff between the convergence and exploration–exploitation, and to control the particle's velocity. However, the search space also matters when selecting these parameters. The values have been tabulated in Table IV. The efficacy of the proposed scheme can be described in terms of the success rate and average time spent in localization. We have considered separate scenarios for localization under the influence of a time-varying disturbance and localization in the absence of external perturbations. These cases are further branched into localization via MASs consensus and that via MASs formation. Thus, there are a total of four scenarios in which the investigation is done in this paper (see Table I). Table II presents the median localization time along with the controller implementation technique and success rate for 50 runs of the experiment. We see that only those techniques have a poor success rate which use PSO as their main controller. This is due to several reasons. PSO is just a *proportional-only* control that limits the operating region between the global and the local best. These techniques drastically fail in scenarios with tight constraints on communication as they heavily rely on complete swarm information and consume more energy during the search. Success rates of BBPSO-, APF-PSO-, and P-PSO-based techniques are highly competitive but they are time intensive. FTMCS is a robust finite-time technique with a success rate of 100% but its implementation on a time-triggered basis results in suboptimal utilization of available resources. For time-triggered implementation of our scheme, the control protocol (23) has been used. The same protocol has been scheduled in an event-triggered manner using (17). Figs. 4 and 5 depict the average localization time for the four scenarios under different implementations of the same protocol.

Depending on the condition (31), samples are taken and the controller is updated with a new value. Between successive sampling instants, the controller is relaxed and runs open loop.

Let us define the sampling interval for the ith agent as $T_i^h = t_i^{h+1} - t_i^h$. The computational cost is given in terms of the number of control updates, or the amount of signal samples that reach the actuator from the sensors. For this, we have taken 1000 samples in 10 s for a time-triggered case, against which we shall compare the efficiency of the proposed event-driven scheme. Fig. 6 illustrates the sampling intervals of the agents under event-triggered sampling. The comparison shows the effective reduction in the number of control signal updates in the event-driven case. From the data, we can see that for 100 updates in the time-triggered case, only 30 updates are needed in the event-triggered case. This is a drastic resource saving in terms of control updates alone. It is evident that although fewer samples have been taken and the controller is relaxed at certain instants, the closed-loop response has not been compromised. The total number of controller updates has been tabulated in Table III. Usually, agents communicate over wireless channels, and reducing the number of samples over the channel has a direct impact on the energy efficiency of the network. The energy efficiency can also be correlated with the number of controller updates presented in Table III. Alternately, we can say that the amount of information that reaches the actuators from the sensors has been reduced.

V. CONCLUSION

In this paper, consensus-based odor source localization (OSL) by the MASs under resource constraints has been discussed. Information on wind and odor concentration has been used in predicting the probable location of the source. A hierarchical scheme has been exercised by incorporating group decision making and robust cooperative control to locate the source of odor in a turbulent environment. The control design technique is based on event-triggered SMC that retains the

robustness of SMC while significantly reducing the expenses on available resources, such as bandwidth and energy. The control delivers well in a turbulence-dominated environment and is insensitive to a particular class of uncertainty. For cases of localization via consensus and localization via parallel formation, numerical simulations establish efficacy of the scheme proposed in this paper. The localization is not only completed in much less time compared to other existing strategies but the success rate of 100 percent is also guaranteed. In the future, we shall try to address the localization of multiple sources under switching topologies and data packet dropout.

REFERENCES

[1] G. Kowadlo and R. A. Russell, "Robot odor localization: A taxonomy and survey," *Int. J. Robot. Res.*, vol. 27, no. 8, pp. 869–894, 2008. doi: 10.1177/0278364908095118.

[2] G. S. Settles, "Sniffers: Fluid-dynamic sampling for olfactory trace detection in nature and homeland security—The 2004 Freeman scholar lecture," *J. Fluids Eng.*, vol. 127, no. 2, pp. 189–218, Feb. 2005. doi: 10.1115/1.1891146.

[3] D. W. Gage, "Many-robot MCM search systems," in *Proc. Auton. Veh. Mine Countermeasures Symp.*, 1995, pp. 9–55.

[4] H. Ishida, T. Nakamoto, T. Moriizumi, T. Kikas, and J. Janata, "Plume-tracking robots: A new application of chemical sensors," *Biol. Bull.*, vol. 200, no. 2, pp. 222–226, 2001. [Online]. Available: https://doi.org/10.2307/1543320

[5] J. A. Farrell, S. Pang, and W. Li, "Plume mapping via hidden Markov methods," *IEEE Trans. Syst., Man, Cybern. B, Cybern.*, vol. 33, no. 6, pp. 850–863, Dec. 2003.

[6] M. Vergassola, E. Villermaux, and B. Shraiman, "'Infotaxi' as a strategy for searching without gradients," *Nature*, vol. 445, no. 7126, pp. 406–409, 2007. [Online]. Available: https://hal.archives-ouvertes.fr/hal-00326807

[7] A. Sinha, R. Kaur, R. Kumar, and A. P. Bhondekar, "Cooperative control of multi-agent systems to locate source of an odor," *ArXiv e-prints*, Nov. 2017. [Online]. Available: http://adsabs.harvard.edu/abs/2017arXiv171103819S

[8] Q. Lu, Q.-L. Han, X. Xie, and S. Liu, "A finite-time motion control strategy for odor source localization," *IEEE Trans. Ind. Electron.*, vol. 61, no. 10, pp. 5419–5430, Oct. 2014.

[9] X. Cui, C. T. Hardin, R. K. Ragade, and A. S. Elmaghraby, "A swarm approach for emission sources localization," in *Proc. 16th IEEE Int. Conf. Tools Artif. Intell.*, Nov. 2004, pp. 424–430.

[10] A.-Q. Hoang and M.-T. Pham, "Swarm intelligence-based approach for macroscopic scale odor source localization using multi-robot system," in *Advances in Information and Communication Technology*, M. Akagi, T.-T. Nguyen, D.-T. Vu, T.-N. Phung, and V.-N. Huynh, Eds. Cham, Switzerland: Springer Int., 2017, pp. 593–602.

[11] R. A. Krohling and E. Mendel, "Bare bones particle swarm optimization with Gaussian or Cauchy jumps," in *Proc. IEEE Congr. Evol. Comput.*, May 2009, pp. 3285–3291.

[12] C. Lytridis, G. S. Virk, Y. Rebour, and E. E. Kadar, "Odor-based navigational strategies for mobile agents," *Adapt. Behav.*, vol. 9, nos. 3–4, pp. 171–187, Apr. 2001. doi: 10.1177/10597123010093004.

[13] R. Rozas, J. Morales, and D. Vega, "Artificial smell detection for robotic navigation," in *Proc. 5th Int. Conf. Adv. Robot. Unstruct. Environ. (ICAR)*, vol. 2, Jun. 1991, pp. 1730–1733.

[14] V. Genovese, P. Dario, R. Magni, and L. Odetti, "Self organizing behavior and swarm intelligence in a pack of mobile miniature robots in search of pollutants," in *Proc. IEEE/RSJ Int. Conf. Intell. Robots Syst.*, vol. 3, Jul. 1992, pp. 1575–1582.

[15] L. Buscemi, M. Prati, and G. Sandini, "Cellular robotics: Behaviour in polluted environments," in *Proc. 2nd Int. Symp. Distrib. Auton. Robot. Syst.*, 1994.

[16] M. H. E. Larcombe, *Robotics in Nuclear Engineering: Computer Assisted Teleoperation in Hazardous Environments With Particular Reference to Radiation Fields*. London, U.K.: Graham and Trotman, 1984.

[17] R. A. Russell, A. Bab-Hadiashar, R. L. Shepherd, and G. G. Wallace, "A comparison of reactive robot chemotaxis algorithms," *Robot. Auton. Syst.*, vol. 45, no. 2, pp. 83–97, 2003. [Online]. Available: http://www.sciencedirect.com/science/article/pii/S0921889003001209

[18] S. Pang and J. A. Farrell, "Chemical plume source localization," *IEEE Trans. Syst., Man, Cybern. B, Cybern.*, vol. 36, no. 5, pp. 1068–1080, Oct. 2006.

[19] D. F. Spears, D. R. Thayer, and D. Zarzhitsky, "Physics-based approach to chemical source localization using mobile robotic swarms," Ph.D. dissertation, Dept. Comput. Sci., Univ. Wyoming, Laramie, WY, USA, 2008.

[20] W. Ren and R. W. Beard, "Consensus seeking in multiagent systems under dynamically changing interaction topologies," *IEEE Trans. Autom. Control*, vol. 50, no. 5, pp. 655–661, May 2005.

[21] W. Yu, G. Chen, W. Ren, J. Kurths, and W. X. Zheng, "Distributed higher order consensus protocols in multiagent dynamical systems," *IEEE Trans. Circuits Syst. I, Reg. Papers*, vol. 58, no. 8, pp. 1924–1932, Aug. 2011.

[22] M. L. Cao, Q. H. Meng, Y. X. Wu, M. Zeng, and W. Li, "Consensus based distributed concentration-weighted summation algorithm for gas-leakage source localization using a wireless sensor network," in *Proc. 32nd Chinese Control Conf.*, Jul. 2013, pp. 7398–7403.

[23] G. Sandini, G. Lucarini, and M. Varoli, "Gradient driven self-organizing systems," in *Proc. IEEE/RSJ Int. Conf. Intell. Robots Syst. (IROS)*, vol. 1, Jul. 1993, pp. 429–432.

[24] A. T. Hayes, A. Martinoli, and R. M. Goodman, "Swarm robotic odor localization: Off-line optimization and validation with real robots," *Robotica*, vol. 21, no. 4, pp. 427–441, Aug. 2003. doi: 10.1017/S0263574703004946.

[25] C. Lytridis, G. Virk, and E. Kadar, "Co-operative smell-based navigation for mobile robots," in *Climbing and Walking Robots*. Heidelberg, Germany: Springer, 2005, pp. 1107–1117.

[26] A. Dhariwal, G. S. Sukhatme, and A. A. G. Requicha, "Bacterium-inspired robots for environmental monitoring," in *Proc. IEEE Int. Conf. Robot. Autom. (ICRA)*, vol. 2, Apr. 2004, pp. 1436–1443.

[27] J. W. Fronczek and N. R. Prasad, "Bio-inspired sensor swarms to detect leaks in pressurized systems," in *Proc. IEEE Int. Conf. Syst. Man Cybern.*, vol. 2, Oct. 2005, pp. 1967–1972.

[28] J. Kennedy and R. Eberhart, "Particle swarm optimization," in *Proc. IEEE Int. Conf. Neural Netw.*, vol. 4, Nov. 1995, pp. 1942–1948.

[29] W. Jatmiko, K. Sekiyama, and T. Fukuda, "A pso-based mobile robot for odor source localization in dynamic advection-diffusion with obstacles environment: Theory, simulation and measurement," *IEEE Comput. Intell. Mag.*, vol. 2, no. 2, pp. 37–51, May 2007.

[30] Q. Lu, S.-R. Liu, and X.-N. Qiu, "A distributed architecture with two layers for odor source localization in multi-robot systems," in *Proc. IEEE Congr. Evol. Comput. (CEC)*, Jul. 2010, pp. 1–7.

[31] Q. Lu and Q.-L. Han, "Decision-making in a multi-robot system for odor source localization," in *Proc. 37th Annu. Conf. IEEE Ind. Electron. Soc. (IECON)*, Nov. 2011, pp. 74–79.

[32] Q. Lu, S. Liu, X. Xie, and J. Wang, "Decision making and finite-time motion control for a group of robots," *IEEE Trans. Cybern.*, vol. 43, no. 2, pp. 738–750, Apr. 2013.

[33] A. Sinha, R. Kumar, R. Kaur, and A. P. Bhondekar, "Consensus-based odor source localization by multiagent systems," *IEEE Trans. Cybern.*, to be published. doi: 10.1109/TCYB.2018.2869224.

[34] Q. Lu and Q.-L. Han, "A probability particle swarm optimizer with information-sharing mechanism for odor source localization," *IFAC Proc. Vol.*, vol. 44, no. 1, pp. 9440–9445, 2011. [Online]. Available: http://www.sciencedirect.com/science/article/pii/S1474667016451281

[35] J. A. Farrell, J. Murlis, X. Long, W. Li, and R. T. Cardé, "Filament-based atmospheric dispersion model to achieve short time-scale structure of odor plumes," *Environ. Fluid Mech.*, vol. 2, no. 1, pp. 143–169, Jun. 2002. [Online]. Available: https://doi.org/10.1023/A:1016283702837

[36] A. Sinha and R. K. Mishra, "Temperature regulation in a continuous stirred tank reactor using event triggered sliding mode control," *IFAC-PapersOnLine*, vol. 51, no. 1, pp. 401–406, 2018. [Online]. Available: https://www.sciencedirect.com/science/article/pii/S2405896318302210

[37] A. Sinha and R. K. Mishra, "Control of a nonlinear continuous stirred tank reactor via event triggered sliding modes," *Chem. Eng. Sci.*, vol. 187, pp. 52–59, Sep. 2018. [Online]. Available: http://www.sciencedirect.com/science/article/pii/S0009250918302719

[38] C. Edwards and S. K. Spurgeon, *Sliding Mode Control: Theory and Applications*. Boca Raton, FL, USA: CRC, 1998.

[39] K. D. Young, V. I. Utkin, and U. Ozguner, "A control engineer's guide to sliding mode control," *IEEE Trans. Control Syst. Technol.*, vol. 7, no. 3, pp. 328–342, May 1999.

[40] F. R. K. Chung, *Spectral Graph Theory* (CBMS Regional Conference Series in Mathematics), vol. 92. Providence, RI, USA: AMS, 1997. [Online]. Available: http://bookstore.ams.org/cbms-92

[41] E. D. Sontag, *Input to State Stability: Basic Concepts and Results*. Heidelberg, Germany: Springer, 2008, pp. 163–220. [Online]. Available: https://doi.org/10.1007/978–3-540–77653-6_3
[42] A. Loutfi, S. Coradeschi, L. Karlsson, and M. Broxvall, "Putting olfaction into action: Using an electronic nose on a multi-sensing mobile robot," in *Proc. IEEE/RSJ Int. Conf. Intell. Robots Syst. (IROS)*, vol. 1, Sep. 2004, pp. 337–342.
[43] Q. Lu and Q.-L. Han, "A finite-time particle swarm optimization algorithm," in *Proc. IEEE Congr. Evol. Comput.*, Jun. 2012, pp. 1–8.
[44] M. Guo and D. V. Dimarogonas, "Nonlinear consensus via continuous, sampled, and aperiodic updates," *Int. J. Control*, vol. 86, no. 4, pp. 567–578, 2013. doi: 10.1080/00207179.2012.747735.
[45] E. Garcia, Y. Cao, and D. W. Casbeer, "An event-triggered control approach for the leader-tracking problem with heterogeneous agents," *Int. J. Control*, vol. 91, no. 5, pp. 1209–1221, 2018. doi: 10.1080/00207179.2017.1312668.
[46] A. Sinha and R. K. Mishra, "Consensus in first order nonlinear heterogeneous multi-agent systems with event-based sliding mode control," *Int. J. Control*, pp. 1–14, Oct. 2018. doi: 10.1080/00207179.2018.1531147.
[47] R. K. Mishra and A. Sinha, "Event-triggered sliding mode based consensus tracking in second order heterogeneous nonlinear multi-agent systems," *Eur. J. Control*, vol. 45, pp. 30–44, Jan. 2019. [Online]. Available: http://www.sciencedirect.com/science/article/pii/S0947358017303187
[48] M. Heymann, F. Lin, G. Meyer, and S. Resmerita, "Analysis of Zeno behaviors in a class of hybrid systems," *IEEE Trans. Autom. Control*, vol. 50, no. 3, pp. 376–383, Mar. 2005.
[49] J. Zhang, K. H. Johansson, J. Lygeros, and S. Sastry, "Zeno hybrid systems," *Int. J. Robust Nonlinear Control*, vol. 11, no. 5, pp. 435–451, 2001. [Online]. Available: https://onlinelibrary.wiley.com/doi/abs/10.1002/rnc.592
[50] J. Matthes, L. Groll, and H. B. Keller, "Source localization by spatially distributed electronic noses for advection and diffusion," *IEEE Trans. Signal Process.*, vol. 53, no. 5, pp. 1711–1719, May 2005.
[51] L. Marques, U. Nunes, and A. T. de Almeida, "Particle swarm-based olfactory guided search," *Auton. Robots*, vol. 20, no. 3, pp. 277–287, Jun. 2006. [Online]. Available: https://doi.org/10.1007/s10514-006-7567-0

Abhinav Sinha (M'19) received the B.Tech. degree in electronics and instrumentation engineering from the Kalinga Institute of Industrial Technology, Bhubaneswar, India, in 2014 and the M.Tech. degree in mechatronics from the Indian Institute of Engineering Science and Technology Shibpur, Howrah, India, in 2018. He is currently pursuing the Doctoral degree with the Intelligent Systems and Control Laboratory, Department of Aerospace Engineering, Indian Institute of Technology Bombay, Mumbai.

From 2014 to 2016, he was an Assistant System Engineer with the Engineering and Industrial Services Division, Tata Consultancy Services (TCS) Ltd., Pune, India, where he worked on control system integration, manufacturing execution systems, enterprise manufacturing intelligence, network segmentation, data integration, and data security at the plant level. He was also a Visiting Faculty Member with TCS, Global Learning Centre, Trivandrum, India, in 2015. From 2017 to 2018, he was a Graduate Researcher with the CSIR-Central Scientific Instruments Organization, Chandigarh, India. His current research interests include sliding-mode control, event-based control, multiagent systems, cooperative control, and cyber-physical systems.

Mr. Sinha was a recipient of the IEEE Best Paper Award from IEEE Pune Section and IEEE Computer Society in 2015, On the Spot Award from TCS in 2015, and the Champions of Initial Learning Programme at TCS in 2015. He is a member of the Automatic Control and Dynamical Optimization Society of the International Federation of Automatic Control.

Ritesh Kumar received the B.E. degree in computer science and engineering from the Manipal Institute of Technology, Manipal, India, in 2009, and the M.Tech. degree in advanced instrumentation and the Ph.D. degree from the Academy of Scientific and Innovative Research, New Delhi, India, in 2011 and 2017, respectively.

Since 2011, he has been a Scientist with the CSIR-Central Scientific Instruments Organization, Chandigarh, India, researching a number of government and industry-sponsored projects involving various domains of information and communication technology, where he is also responsible for supervising lab and tutorials on machine learning. He has authored and coauthored multiple journal papers. His current research interests include big data analytics, perception modeling, and artificial intelligence.

Dr. Kumar is a member of the Digital Olfaction Society and the Institution of Electronics and Telecommunication Engineers.

Rishemjit Kaur received the B.E. degree in electronics (instrumentation and control) from Thapar University, Bhubaneswar, India, in 2009, and the M.Tech. degree in advanced instrumentation and the Ph.D. degree from the Academy of Scientific and Innovative Research, New Delhi, India, in 2011 and 2017, respectively.

Since 2011, she has been a Scientist with the CSIR-Central Scientific Instruments Organization, Chandigarh, India. She was a Research Scholar with Nagoya University, Nagoya, Japan, from 2014 to 2016. She received the Japanese Government Scholarship for research students (MEXT) in 2014–2016. Her current research interests include evolutionary optimization techniques, big data analytics, social network analysis, and machine learning.

Dr. Kaur was a recipient of the Genetic and Evolutionary Computation Conference Virtual Creatures Award for her research on developing controller for soft-bodied robots.

Rajiv Kumar Mishra received the B.Tech. degree in instrumentation and control engineering from the Academy of Technology, Hooghly, India, in 2009 and the M.Tech. degree in instrumentation and electronics engineering from Jadavpur University, Kolkata, India, in 2011. He is currently pursuing the Ph.D. degree in computer science from the Tokyo Institute of Technology, Tokyo, Japan.

From 2011 to 2018, he was an Assistant Professor with the Department of Electronics and Instrumentation Engineering, National Institute of Science and Technology, Berhampur, India, and also with the School of Electronics Engineering, Kalinga Institute of Industrial Technology, Bhubaneswar, India. His current research interests include sliding-mode control, multiagent systems, event-triggered coordination, and networked control.

Mr. Mishra was a recipient of the Japanese Government (MEXT) Scholarship.